Chinese Journal of
POLYMER SCIENCE

ARTICLE

https://doi.org/10.1007/s10118-020-2361-6
Chinese J. Polym. Sci. **2020**, *38*, 298–310

The Crystallization and Melting Behaviors of PDLA-*b*-PBS-*b*-PDLA Tri-block Copolymers

Cong-Shu Feng[a], Yun Chen[a], Jun Shao[a,b*], Gao Li[c], and Hao-Qing Hou[a*]

[a] *College of chemistry and chemical engineering, Jiangxi Normal University, Nanchang 330022, China*
[b] *Jiangxi Key Laboratory of Organic Chemistry, Jiangxi Science and Technology Normal University, Nanchang 330013, China*
[c] *Key Laboratory of Polymer Ecomaterials, Changchun Institute of Applied Chemistry, Chinese Academy of Sciences, Changchun 130022, China*

Electronic Supplementary Information

Abstract In this study, the poly(D-lactide)-block-poly(butylene succinate)-block-poly(D-lactide) (PDLA-*b*-PBS-*b*-PDLA) triblock copolymers with a fixed length of PBS and various lengths of PDLA are synthesized, and the crystallization behaviors of the PDLA and PBS blocks are investigated. Although both the crystallization behaviors of PBS and PDLA blocks depend on composition, they exhibit different variations. For the PDLA block, its crystallization behaviors are mainly influenced by temperature and block length. The crystallization signals of PDLA block appear in the B-D 2-2 specimen, and these signals get enhanced with PDLA block length. The crystallization rates tend to decrease with increasing PDLA block lendth during crystallizing at 90 and 100 °C. Crystallizing at higher temperature, the crystallization rates increase at first and then decrease with block length. The crystallization rates decrease as elevating the crystallization temperature. The melting temperatures of PDLA blocks increase with block lengths and crystallization temperatures. For the PBS block, its crystallization behaviors are mainly controlled by the nucleation and confinement from PDLA block. The crystallization and melting enthalpies as well as the crystallization and melting temperatures of PBS block reduce as a longer PDLA block has been copolymerized, while the crystallization rates of the PBS block exhibit unique component dependence, and the highest rate is observed in the B-D 2-2 specimen. The Avrami exponent of PBS crystallites is reduced as a longer PDLA block is incorporated or the sample is crystallized at higher temperature. This investigation provides a convenient route to tune the crystallization behavior of PBS and PLA.

Keywords Poly(butylenes succinate) (PBS); Poly(D-lactide) (PDLA); Poly(D-lactide)-block-PBS-block-poly(D-lactide) (PDLA-*b*-PBS-*b*-PDLA); Crystallization behavior

Citation: Feng, C. S.; Chen, Y.; Shao, J.; Li, G.; Hou, H. Q. The crystallization and melting behaviors of PDLA-*b*-PBS-*b*-PDLA tri-block copolymers. *Chinese J. Polym. Sci.* **2020**, *38*, 298–310.

INTRODUCTION

In the twenty first century, the environmental problems such as fog and haze weather, air contamination, and soil and water pollutions are becoming bad to worse. Most of these pollutions relate to the consumption of non-renewable resources, *i.e.*, crude oil, coal, and natural gas. These non-reproducible resources not only provide fuel and energy, but also supply raw material for producing most traditional non-biodegradable polymers.[1] In the field of polymer material, seeking for the one that originates from bio-based sources and affords biodegradable products to replace the traditional non-biodegradable polymers has attracted considerable attention. Poly(lactic acid) (PLA) can be produced from recycle sources, its products are biodegradable under natural environment,[2] and PLA materials also exhibit excellent mechanical performance as well as bioresorbable and biocompatible properties. Thus, PLA possesses widespread potential in lots of fields. However, the fragile behavior is one bottleneck to its application.[3–5] Poly(butylene succinate) (PBS) is another biodegradable polyester whose monomers also start from renewable feedstocks. It presents balanced mechanical performance and exhibits wide applications in common used field, medical research, and drug delivery.[6,7] Furthermore, PBS displays excellent ductility behavior in most cases.[8]

Blending of PBS with PLA appears to be an ideal route to property improvement of these two polymers because their complementarities could promote the toughness of PLA and the stiffness of PBS. However, a key factor in determining the success of blending these two polymers is the extent of miscibility. Although Wuk and Soon declared that PLA and PBS are fully miscible through calculating the Flory-Huggins interaction parameter,[9] morphological, rheological, and thermal analyses revealed that PBS and PLA are immiscible.[10–12] Lots of technologies are adopted to enhance the performance of PLA/PBS blends, such as maleation,[13] adding organoclay,[14]

* Corresponding authors, E-mail: jun.shao@jxnu.edu.cn (J.S.)
E-mail: hhq2001911@126.com (H.Q.H.)

Received June 11, 2019; Accepted October 8, 2019; Published online November 27, 2019

uniaxial stretching,[15] incorporating grafted copolymer,[16] coupling,[17] and crosslinking.[18,19] Most of these attempts have improved the properties of PLA/PBS blends successfully. In addition, block copolymer is an effective compatibilizer for the immiscible mixtures, which is better than random copolymer.[20,21] In a previous study, the poly(D-lactide)-block-PBS-block-poly(D-lactide) (PDLA-*b*-PBS-*b*-PDLA) triblock copolymers supplied ductility at a specific content when they were incorporated into poly(lactide) with L-configuration (PLLA).[22] Although the crystallization behaviors of PLA,[5,23–25] PBS,[26–28] and PLA/PBS blends[11,12,29,30] have been investigated in various aspects, and the chemical syntheses and physical characterizations of poly(lactide-*b*-butylene succinate-*b*-lactide) (PLA-*b*-PBS-*b*-PLA) triblocks[31–33] and multiblocks have also been reported,[34] the crystallization and melting behaviors of the PLA-*b*-PBS-*b*-PLA block copolymers have not been investigated in detail yet.

In the PLA-*b*-PBS-*b*-PLA tri-block copolymers, both PLA and PBS blocks could develop crystallites at proper environment. For a double crystalline block copolymer, the effects of one block on the crystallization behavior and morphology of the second one are interesting, complicated, but important, which involve several factors, such as composition, segment sequence, miscibility, and thermal treatment history.[35,36] In the case of double crystalline block copolymer with different crystallization conditions, the second block could be nucleated, or its crystallization could be confined within the microdomain structure or within the previously formed lamellar stacks of the first block;[37,38] then, copolymers with different morphologies, mechanical properties, and biomedical and engineering applications could be produced. Accordingly, the block copolymer provides a facilitate approach to tailor the performance of materials. Unfortunately, the crystallization behaviors of PLA and PBS blocks, and the mutual effects of the PBS and PLA segments in the PLA-*b*-PBS-*b*-PLA triblock copolymers have not been elaborated clearly till now. For this purpose, a series of PDLA-*b*-PBS-*b*-PDLA triblock copolymers with fixed length of PBS and different lengths of PDLA were synthesized in this study, and the crystallization behaviors of PBS and PDLA blocks were separately investigated. Results indicated that the crystallization rate of PDLA block was depressed after copolymerization, while the crystallization of PBS block was influenced by the nucleation and confinement of PDLA crystallites preformed at the first stage. This investigation would supply more bases for the study of double crystalline block copolymers.

EXPERIMENTAL

Materials

Tetrabutyl titanate ($Ti(OBu)_4$, ≥ 98%) and tin(II) 2-ethylhexanoate ($Sn(Oct)_2$, > 95%) were purchased from Aladdin. 1,4-Butanediol, succinic acid, ethyl acetate, ethanol, and dichloromethane were from domestic agents with a purity of analytical grade. Ethyl acetate was refluxed under calcium hydride for 24 h before distillation. The dextrorotatory-lactide, dimer of lactic acid with D configuration, (D-LA, ≥ 99.5%) was purchased from Changchun SinoBiomaterials (China) and recrystallized in anhydrous ethyl acetate for three times before use. All the other agents were used directly as received.

Synthesis of PBS

The synthesis routes to PBS and PDLA-*b*-PBS-*b*-PDLA are presented in Scheme 1. For the synthesis of PBS, 1.0 mol of succinic acid, 1.2 mol of 1,4-butanediol, and 0.02 mol of $Ti(OBu)_4$ were reacted at 190 °C under nitrogen atmosphere. When no more water was distilled out, the polycondensation was kept at 220–240 °C under a vacuum of 70 Pa for 20 h.[39] The raw PBS product was dissolved in dichloromethane and precipitated with an excess amount of cold ethanol. The purification was repeated twice. The final powder product was dried to constant weight at 80 °C under vacuum.

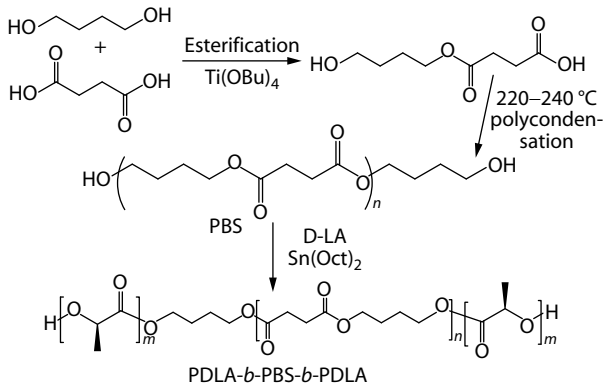

Scheme 1 The synthesis routes to PBS and PDLA-*b*-PBS-*b*-PDLA copolymers.

Synthesis of PDLA-*b*-PBS-*b*-PDLA

The PDLA-*b*-PBS-*b*-PDLA copolymers were synthesized *via* ring-opening polymerization of D-LA monomers as references.[33,34,40] Dihydroxyl-capped PBS and $Sn(Oct)_2$ were employed as the macro-initiator and catalyst, respectively. PBS, $Sn(Oct)_2$, and D-LA were mixed and heated up to 80 °C and vacuumed for 2 h to completely eliminate the moisture. The copolymerization was implemented at 120 °C in bulk for 24 h under nitrogen atmosphere. The products were purified by pouring their dichloromethane solution into ethanol. The copolymers were dried at 80 °C in vacuum for 72 h. Copolymers with different block lengths were regulated by weight ratio of PBS/D-LA. Characterizations of PBS and the copolymers are listed in Table S1 (in the electronic supplementary information, ESI).

Characterizations

Nuclear magnetic resonance spectroscopy (NMR) was performed on a Bruker AV 300 MHz spectrometer in $CDCl_3$, and tetramethylsilane (TMS) was used as an internal reference. The ^{1}H-NMR spectra of PBS and B-D 2-2 specimen are shown in Fig. S1 (in ESI).

The number-average molecular weight (M_n) and polydispersity indexes (PDI) of polymers were evaluated in chloroform by using gel permeation chromatography (GPC, Waters, USA) with two Styragel® HR gel columns (HR2 and HR4). The GPC device was a Waters HPLC system equipped with a Waters 2515 pump and a refractive index detector. The flow rate of eluent was 1 mL/min at 35 °C. Monodispersed polystyrene standards (Waters, USA) with molecular weights ranging from 1790 to 64.2 × 10^4 were used to generate the calibration curve. M_n and PDI of PBS and copolymers are listed in Table

https://doi.org/10.1007/s10118-020-2361-6

S1 (in ESI).

Wide-angle X-ray diffraction (WAXD) was carried out on Bruker D8 Advance X-ray diffractometer equipped with Cu Kα radiation. The measurement ranged from 2θ = 10° to 30° at a scan speed of 2 (°)/min. The WAXD patterns of all the specimens are presented in Fig. S2 (in ESI).

The thermal properties of PBS and PDLA-*b*-PBS-*b*-PDLA copolymers were examined by differential scanning calorimetry (DSC) (Q100, TA Instruments, USA). The temperature and heat flow were calibrated with standard indium. The specimens were heated from –40 °C to 200 °C at a rate of 10 °C/min, and maintained at 200 °C for 5 min to melt all the crystallites completely. For the isothermal protocols, the following steps were adopted: i) cooled to the given temperature (T_{c1}, which was 90, 100, 110, 120, 130, or 140 °C) at a rate of 60 °C/min and kept for 60 min; then cooled to 70 °C (T_{c2}) at a rate of 60 °C/min and kept isothermal for 60 min; finally heated to 200 °C at 10 °C/min; ii) cooled to 130 °C at a rate of 60 °C/min and kept for 60 min (in this stage PDLA could crystallize efficiently in most cases); then cooled to the given temperature, *i.e.*, 70, 75, 80, 85, or 90 °C, at a rate of 60 °C/min and crystallized for 60 min to explore the crystallization of PBS block; finally heated to 200 °C at 10 °C/min. All the measurements were carried out under nitrogen atmosphere.

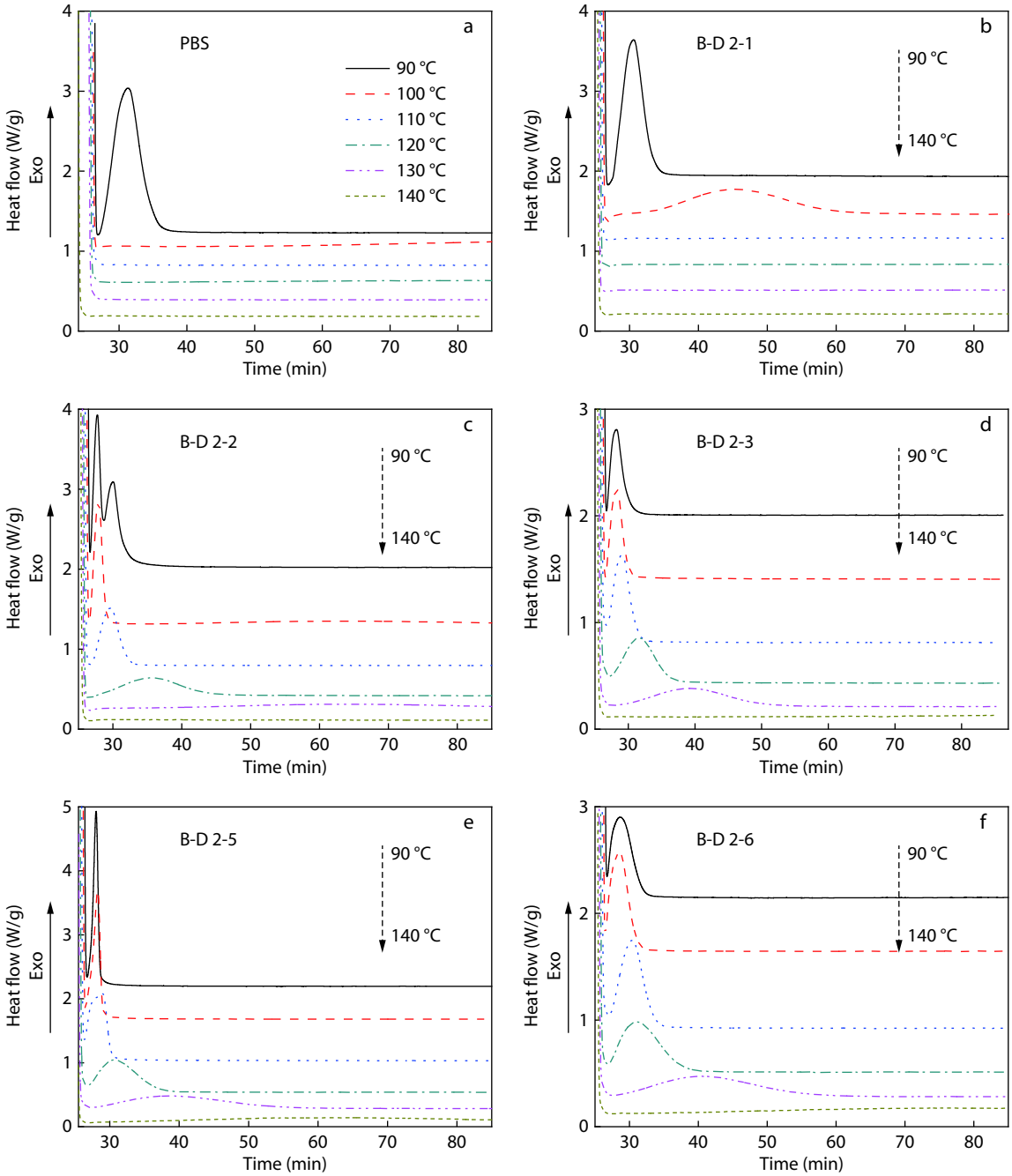

Fig. 1 The isothermal thermograms of PBS (a) and its copolymers (b–f) at 90–140 °C.

https://doi.org/10.1007/s10118-020-2361-6

RESULTS AND DISCUSSION

The Crystallization Behavior of PDLA Block

PBS and PDLA would form crystallites separately during crystallization. The melting temperature of PBS is ~114 °C, while that of PDLA varies from 120 °C to 170 °C with different block lengths in this study (Fig. S3 in ESI). In order to distinguish the crystallization signals of PBS and PDLA blocks, the specimens were firstly isothermally crystallized at 90–140 °C, and the DSC results are presented in Fig. 1. For neat PBS (Fig. 1a), one endothermic peak was found when crystallizing at 90 °C, and no obvious crystallization signal was observed at higher crystallization temperature, which should be due to the melting of PBS at ~114 °C that led to difficult nucleation at that high crystallization temperature or in such a time scale. For the B-D 2-1 specimen (Fig. 1b), clear endothermic signals were observed when the crystallization temperature was 90 and 100 °C; according to the calculation of crystallization and melting enthalpies in the subsequent heating, these signals were ascribed to the crystallization of PBS. The crystallites formed at 100 °C for PBS block were related to the hard PDLA block that reduced the mobility of PBS block, and could facilitate the homogeneous nucleation. In the case of B-D 2-2 specimen (Fig. 1c), two crystallization peaks were observed when the crystallization temperature was 90 °C; the peak appearing at early stage belonged to the crystallization of PDLA block because of its higher degree of supercooling, and the second was ascribed to the crystallization of PBS block. The time-dependent WAXD patterns in Fig. S4 (in ESI) also corroborated this assignment. The crystallization signals assigned to PDLA block got enhanced, while those belonged to PBS became smaller and disappeared with more content of D-LA incorporated (Figs. 1c–1f). For the crystallization of PDLA block in all the specimens, the crystallization curves became flatter and the crystallization time became longer as increasing the crystallization temperature. When the temperature reached 140 °C, crystallization signals in all the specimens were not obvious.

Fig. 2 shows the crystallization enthalpies as a function of time (t) for PDLA block. As can be seen, all the curves have sigmoidal shapes. The time to complete crystallization increased as elevating the crystallization temperature, which indicated that the crystallization rates declined gradually (the half crystallization times ($t_{1/2}$) are listed in Table 1). The crystallization enthalpy of PDLA block increased at first (≤ 130 °C) and then decreased when the crystallization temperature increased from 90 °C to 140 °C. Crystallization at lower temperature meant convenient nucleation; also, the molecular chains and segments did not have enough time to arrange orderly, but developed crystallites by locally regulating their conformation and discharge into lattices nearby. These formed crystallites acted as physical corsslinking points and

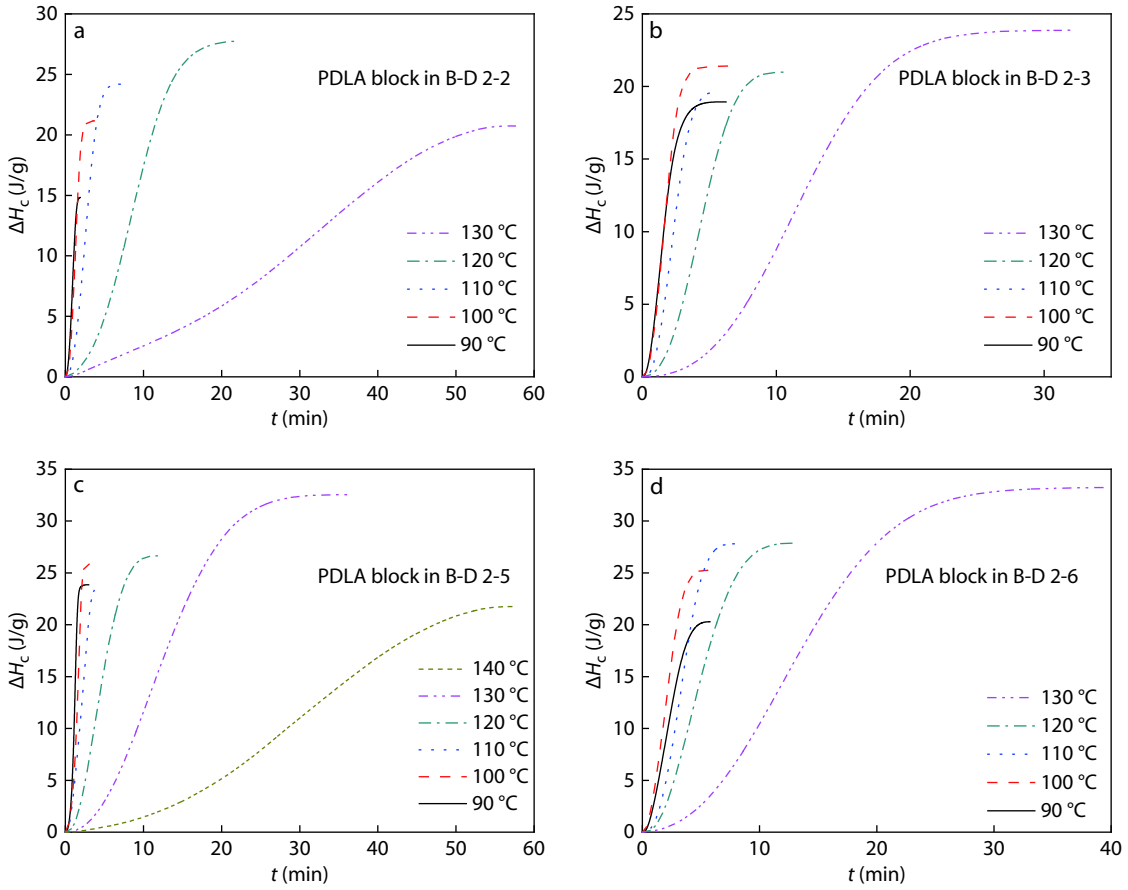

Fig. 2 The crystallization enthalpies (ΔH_c) as a function of crystallization time (t) for PDLA block in B-D 2-2 (a), B-D 2-3 (b), B-D 2-5 (c), and B-D 2-6 (d).

https://doi.org/10.1007/s10118-020-2361-6

confined the movement of amorphous molecular chains and segments around them, leading to lower crystallization enthalpy and thinner lamellae. Increasing crystallization temperature, the crystallization rate reduced as fewer nuclei were developed; the chains and segments exhibited higher mobility and had more time to produce stable crystallites. Thus, a higher content of segments participated in crystallization and thicker lamellae were produced. The decrement of enthalpy at 140 °C should be due to the fact that nucleation was difficult and the crystallization rate was low, so that the PDLA block could not crystallize efficiently at that the high temperature in a limited time period (60 min).

Table 1 Kinetic parameters of isothermal crystallization for PDLA blocks.

Code	Temperature (°C)	n	ln$K$ (min$^{1/n}$)	R^2	$t_{1/2}$ (min)
B-D 2-2	90	2.67	−0.103	0.999	0.91
B-D 2-3		2.14	−1.26	0.999	1.54
B-D 2-5		2.82	−1.10	0.997	1.18
B-D 2-6		2.00	−1.90	0.999	2.20
B-D 2-2	100	2.72	−1.08	0.999	1.30
B-D 2-3		2.23	−1.54	0.999	1.68
B-D 2-5		2.29	−1.67	0.998	1.58
B-D 2-6		1.97	−1.78	0.999	2.05
B-D 2-2	110	2.50	−2.78	0.999	2.64
B-D 2-3		2.64	−2.52	0.999	2.30
B-D 2-5		2.19	−1.85	0.998	2.05
B-D 2-6		2.52	−3.41	0.999	3.33
B-D 2-2	120	2.44	−5.62	0.998	8.12
B-D 2-3		2.39	−3.92	0.999	8.12
B-D 2-5		2.30	−3.75	0.999	4.43
B-D 2-6		2.34	−3.97	0.999	4.80
B-D 2-2	130	2.15	−7.61	0.998	29.34
B-D 2-3		2.51	−6.58	0.999	11.69
B-D 2-5		2.20	−5.89	0.999	12.30
B-D 2-6		2.15	−5.96	0.999	13.06
B-D 2-5	140	1.89	−6.99	0.997	29.80

To investigate the crystallization kinetics of PDLA blocks in detail, Avrami equation was employed to analyze the isothermal crystallization.[41,42] The expression is as follows:

$$1 - X_t = \exp\left[-K(T)\,t^n\right] \quad (1)$$

or

$$\ln\left[-\ln(1 - X_t)\right] = \ln K(T) + n\ln t \quad (2)$$

where X_t is the relative degree of crystallinity at given time (t), X_t could be determined as the ratio between the area of exothermic peak at time t and the total measured area of crystallization. K is the overall kinetic constant and t is the crystallization time. n is the Avrami exponent, which is correlated to the nucleation mechanism and growth dimension. Based on the original assumptions of the theory, n should be an integer, ranging from 1 to 4, corresponding to various growth forms from rod-like to sphere-like, and it also depends on the type of nucleation, *i.e.*, heterogeneous or homogeneous.

The plots of ln[−ln(1 − X_t)] versus ln$t$ for PDLA block are shown in Figs. 3(a)–3(d). In order to avoid the second crystallization which deviated from the straight line, X_t from 3% to

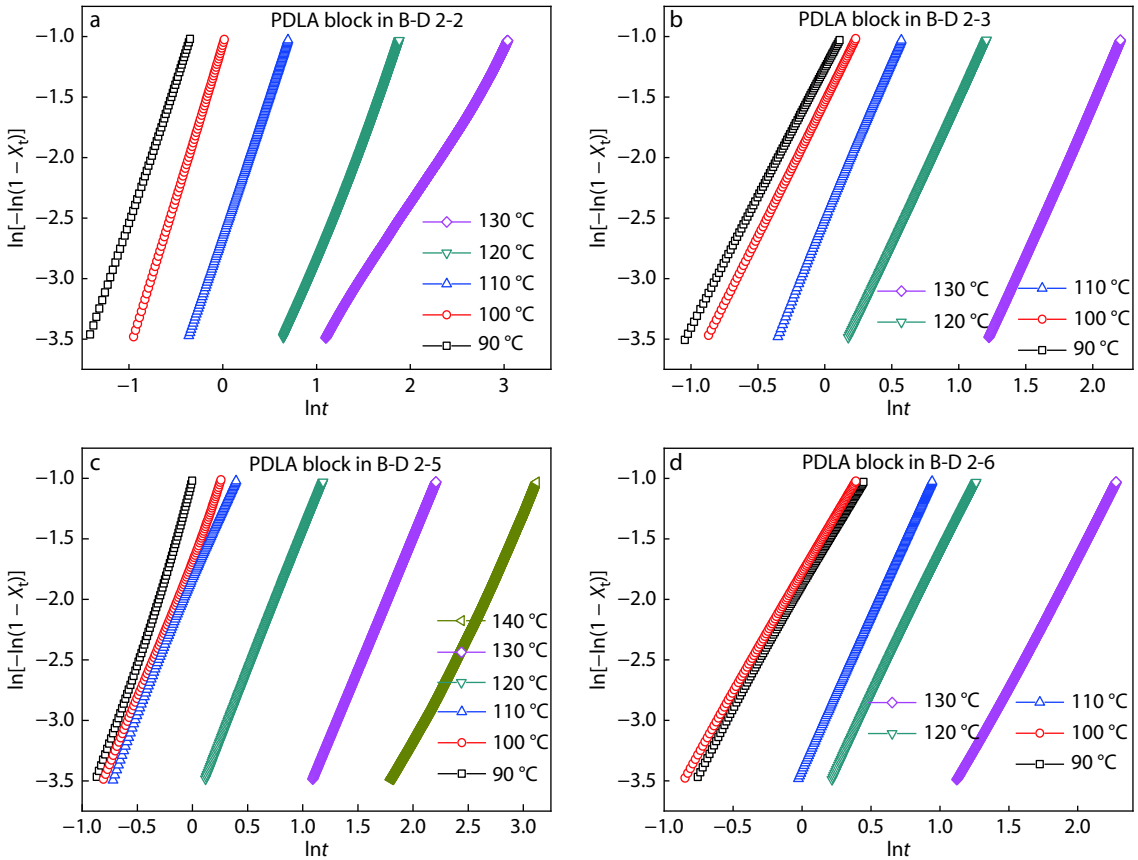

Fig. 3 The plots of ln[−ln(1 − X_t)] versus ln$t$ for PDLA blocks in B-D 2-2 (a), B-D 2-3 (b), B-D 2-5 (c), and B-D 2-6 (d).

https://doi.org/10.1007/s10118-020-2361-6

30% was employed for calculating the slope and intercept for all the specimens.[26,43] It can be seen that all the curves show good linearity. n, ln$K$, and the half crystallization time ($t_{1/2}$) calculated from Figs. 2 and 3 are listed in Table 1. The n values of most PDLA blocks were 2–3, indicating that more than one crystallization mechanisms existed in these copolymers. When the crystallization temperature was higher than 120 °C, the n values reduced gradually, which should be ascribed to changed crystallization mechanisms after temperature elevation, and the crystallites were mainly produced with a two-dimensional structure. It can be seen that ln$K$ declined with increasing isothermal temperature in most of specimens, and $1/t_{1/2}$ presented similar regularity, which suggested that the crystallization rate decreased with the increase of temperature. For different specimens crystallizing at the same temperature, ln$K$ tended to decline with the increasing block length when performing crystallization at 90 and 100 °C. For the PDLA block crystallizing at lower temperatures, nucleation was convenient for all the specimens, and the crystallization rate mainly depended on the motion ability of PDLA seg-

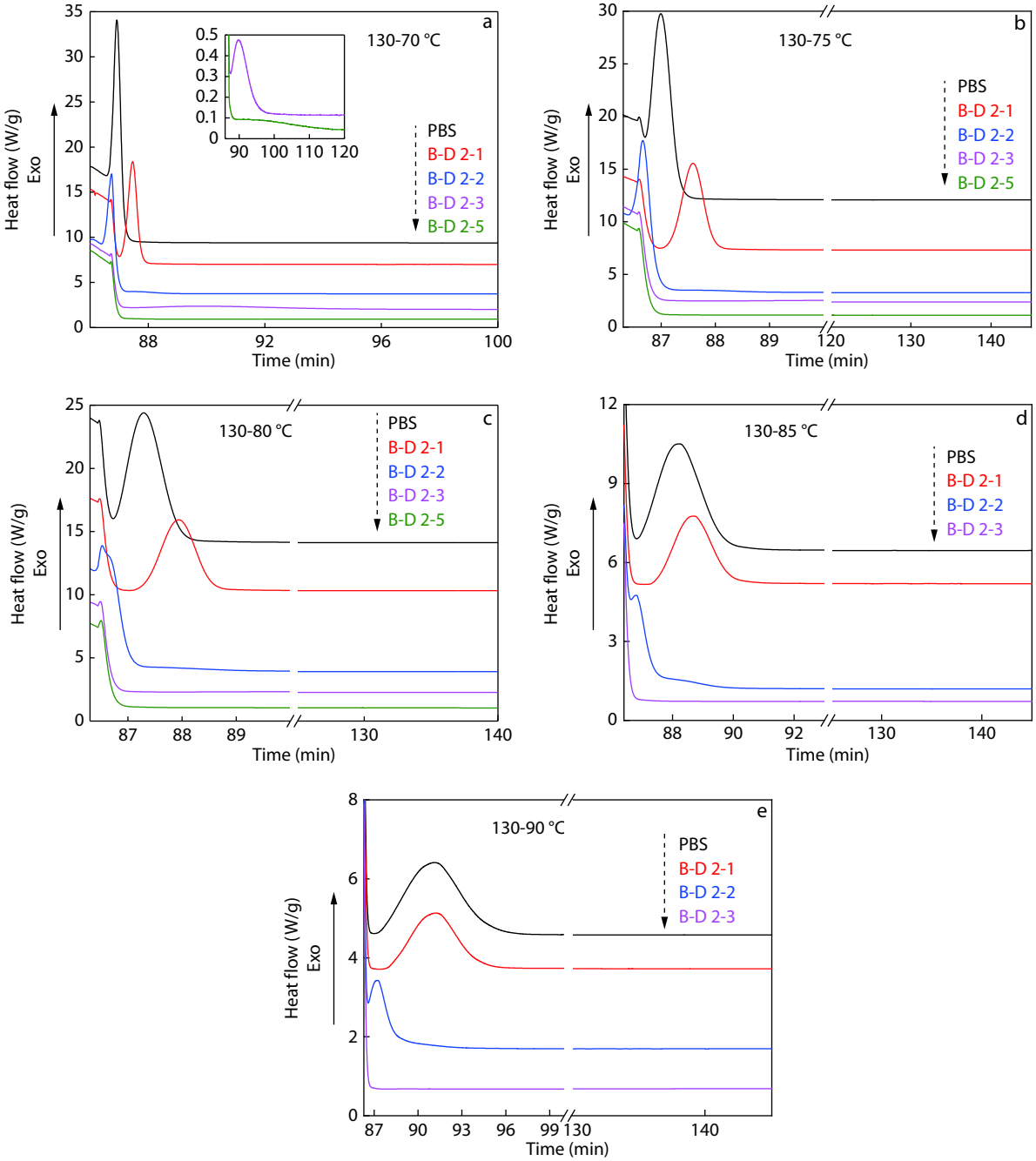

Fig. 4 The isothermal crystallization curves of PBS and its copolymers when crystallized at 130 °C first and then cooled rapidly to 70 °C (a), 75 °C (b), 80 °C (c), 85 °C (d), 90 °C (e).

https://doi.org/10.1007/s10118-020-2361-6

ments. Hence, the copolymer which had shorter PDLA block exhibited higher mobility and crystallized at a faster rate. When the crystallization temperature was above 110 °C, the crystallization rate increased at first and then decreased with the increase of PDLA block length. This diversity at different crystallization temperatures should be ascribed to various crystallization mechanisms at different temperature ranges. At higher crystallization temperature, the motion ability was enhanced for all specimens, and a higher viscosity would facilitate nucleation. However, the higher viscosity also reduced the motion capacity. Accordingly, the specimen with moderate length exhibited the highest crystallization rate.

The Crystallization Behavior of PBS Block

Fig. 2 reveals that the PDLA block crystallized efficiently when crystallized at 130 °C for 60 min in most cases except B-D 2-1. In order to avoid the interruption of PDLA crystallization, all the specimens were crystallized at 130 °C at first, and then were cooled rapidly to 70–90 °C to investigate the crystallization behavior of PBS block. The crystallization curves of PBS block are displayed in Fig. 4. Crystallized at 70 °C, neat PBS had an obvious exothermic peak (Fig. 4a), and the crystallization signals assign-

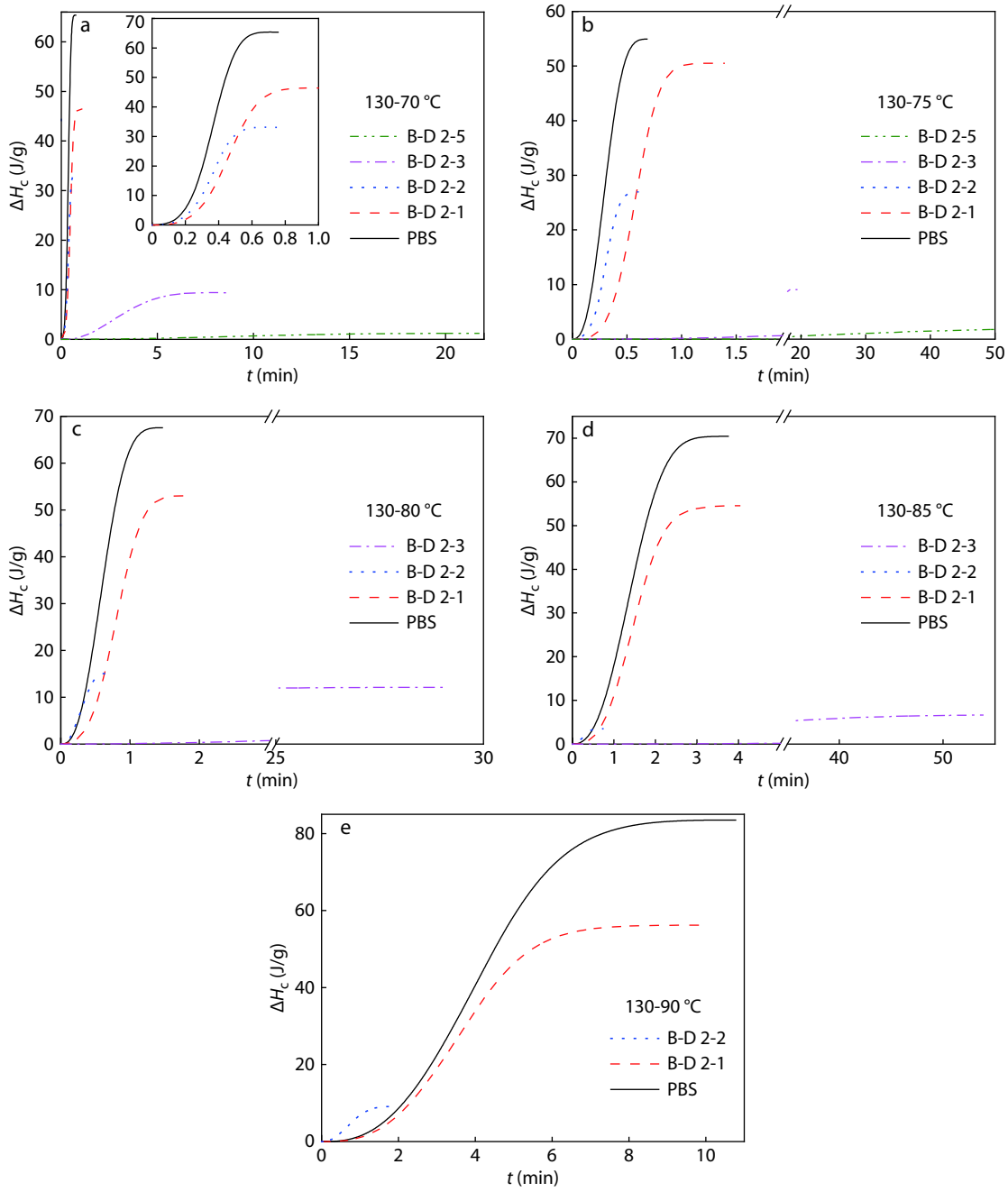

Fig. 5 ΔH_c as a function of t for PDLA-*b*-PBS-*b*-PDLA copolymers crystallized first at 130 °C and then cooled rapidly to 70 °C (a), 75 °C (b), 80 °C (c), 85 °C (d), and 90 °C (e).

https://doi.org/10.1007/s10118-020-2361-6

ed to PBS declined as higher content of PDLA copolymerized. Elevating the crystallization temperature (Figs. 4b–4e), the crystallization peaks assigned to PBS block became flatter, and no obvious exothermic signals were detected in the specimens with the higher D content.

The crystallization enthalpy versus crystallization time and $\ln[-\ln(1-X_t)]$ versus $\ln t$ are presented in Figs. 5 and 6, respectively, and the calculated n, $\ln K$, and $t_{1/2}$ are listed in Table 2. It was found that the crystallization enthalpy of the PBS block reduced after a longer PDLA block was bonded to PBS. For neat PBS and B-D 2-1 specimens, the enthalpy tended to increase when crystallizing at higher temperature. B-D 2-2 exhibited lower crystallization enthalpies as elevating the crystallization temperature, which should be ascribed to its rapid crystallization, and the crystallization peak appeared before cooling to the given temperature (see Fig. 4). All the data coherently indicated that the crystallization rate of PBS block decreased as a small amount of PDLA block was bonded to PBS (B-D 2-1), then increased with a moderate PDLA block length (B-D 2-2), and decreased again for a longer block length of PDLA. When cooling from the melt, B-D 2-2 also presented similar crystallization regularity (Fig. S5 in ESI). This

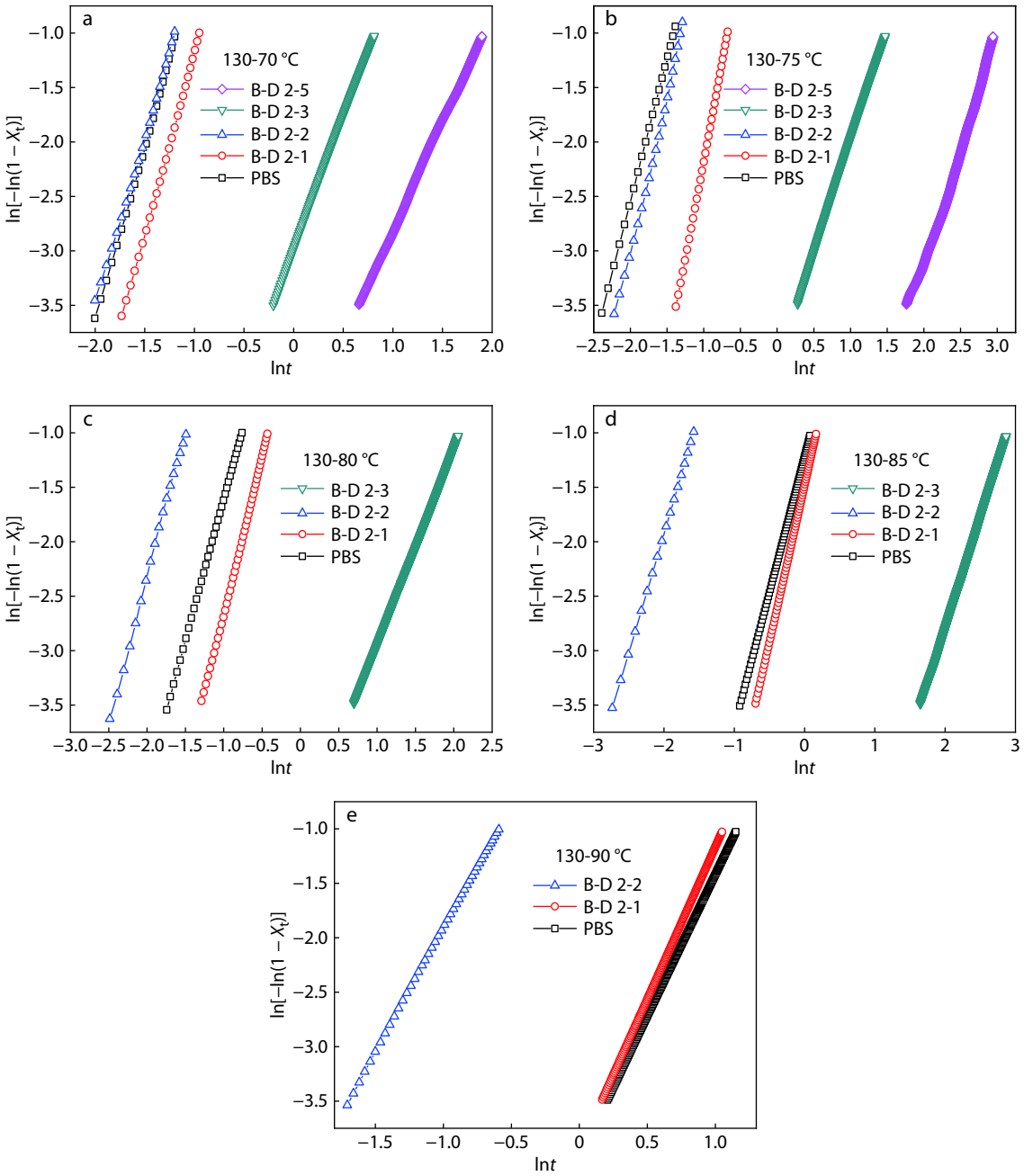

Fig. 6 The plots of $\ln[-\ln(1-X_t)]$ versus $\ln t$ for PBS and its copolymers crystallized first at 130 °C and then cooled rapidly to 70 °C (a), 75 °C (b), 80 °C (c), 85 °C (d), and 90 °C (e).

https://doi.org/10.1007/s10118-020-2361-6

unique variation would be interpreted as that in the copolymers with a short PDLA length, such as B-D 2-1, the PDLA block could not form crystallites. Amorphous PDLA hindered the movement of PBS and thus depressed the crystallization rate. For the PDLA block with a moderate length (B-D 2-2), the PDLA block could form crystallites, and these crystallites supplied lots of nucleate positions for the crystallization of PBS. Although the presence of PDLA block embarrassed the movement of PBS, the nucleation was the major effect, which resulted in a higher crystallization rate. With a longer PDLA block, more nucleate positions would be provided. However, spatial restriction from the PDLA crystallites preformed was more serious and the restriction became the major effect during the crystallization of PBS block. Consequently, the restriction caused the reduction of crystallization rate of the PBS block.

Table 2 Kinetic parameters of isothermal crystallization for PBS blocks.

Code	Temperature (°C)	n	ln$K$ (min^{-1})	R^2	$t_{1/2}$ (min)
PBS	70	3.21	2.77	0.999	0.362
B-D 2-1		3.32	2.13	0.999	0.462
B-D 2-2		3.07	2.65	0.999	0.353
B-D 2-3		2.43	−2.98	0.999	3.03
B-D 2-5		1.99	−4.80	0.999	9.22
PBS	75	2.63	2.71	0.999	0.317
B-D 2-1		3.59	1.41	0.999	0.603
B-D 2-2		2.87	2.72	0.997	0.317
B-D 2-3		2.05	−4.03	0.999	6.27
B-D 2-5		2.14	−7.42	0.994	25.41
PBS	80	2.59	0.983	0.999	0.6
B-D 2-1		2.87	0.201	0.999	0.8
B-D 2-2		2.70	3.07	0.999	0.3
B-D 2-3		1.80	−4.75	0.999	10.92
PBS	85	2.49	−1.22	0.999	1.40
B-D 2-1		2.88	−1.49	0.999	1.47
B-D 2-2		2.19	2.46	0.999	0.265
B-D 2-3		2.04	−6.87	0.999	24.25
PBS	90	2.61	−4.03	0.999	4.06
B-D 2-1		2.79	−3.96	0.999	3.61
B-D 2-2		2.26	0.351	0.999	0.737

As the content of PDLA increased in the copolymer, the n value increased at first and then decreased; the highest n value was found in the B-D 2-1 specimen in all the temperature range. For neat PBS, the crystallites were mainly developed in three dimensional and heterogeneous nucleation dominated the crystallization process at the investigated temperature range. In the B-D 2-1 specimen, the short amorphous PDLA block reduced, and parts of the PBS segments crystallized under homogeneous nucleation condition. Subsequently, a higher n value was obtained. After a higher content of PDLA was incorporated, PDLA would form crystallites at first, and the PBS block crystallized in a restricted environment although the PDLA crystallites provided lots of nucleated positions. This spatial restriction led to the declining of the n value.

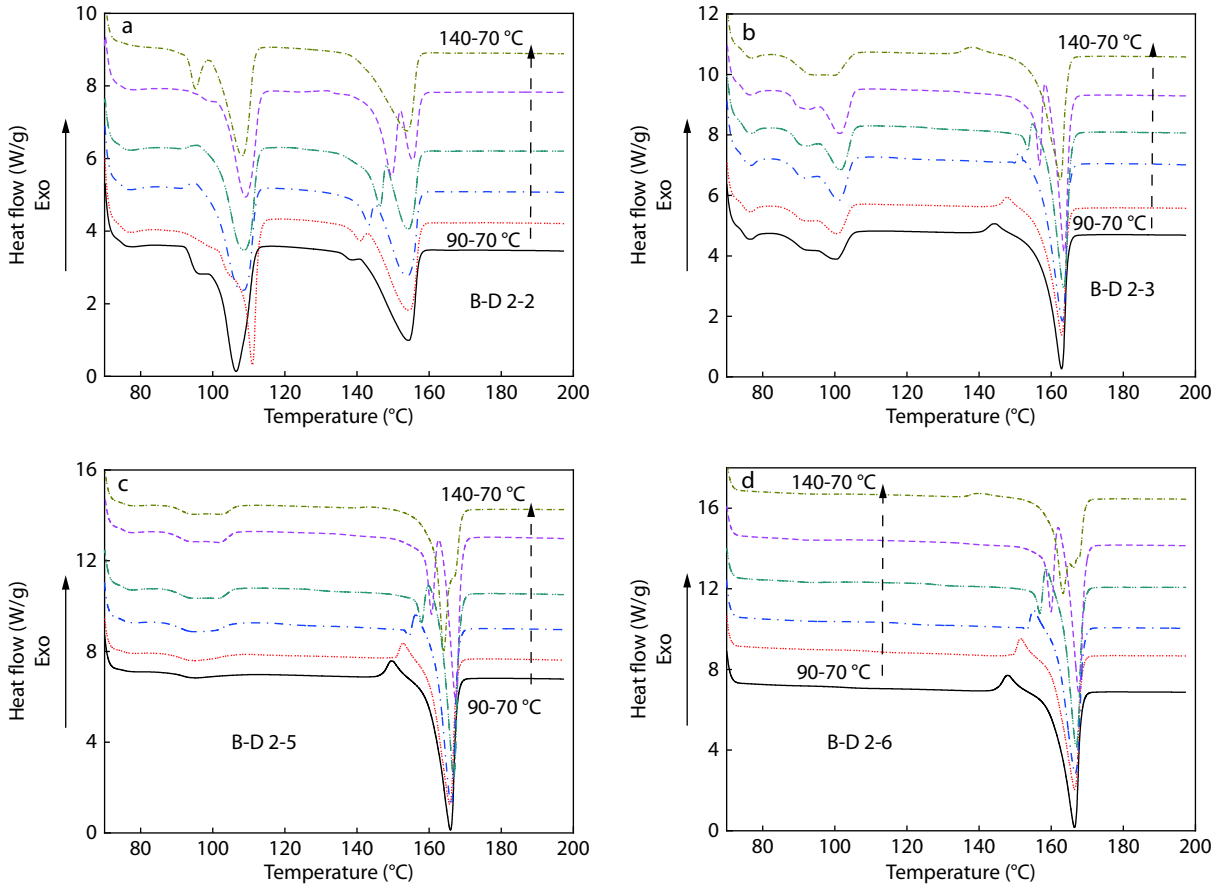

Fig. 7 The second DSC heating curves of B-D 2-2 (a), B-D 2-3 (b), B-D 2-5 (c), and B-D 2-6 (d) after crystallized at 90–140 °C and then at 70 °C.

https://doi.org/10.1007/s10118-020-2361-6

The above results revealed that the crystallization behaviors of PDLA and PBS blocks strongly depended on the composition. For the PDLA block, its crystallization rate was lower than that of PLA homopolymer,[25] while the crystallization of PLA was accelerated in the PLA/PBS blends.[11,29,30] This depression was similar to the poly(ε-caprolactone) (PCL) block in the PLA-*b*-PCL block copolymer[36] but different from the case of PLA-blcok-poly(ethylene glycol) (PLA-*b*-PEG) block copolymer.[44,45] PEG is miscible with PLA in most cases, and it acts as a diluted solvent during the crystallization of PLA block. PCL and PBS blocks are partially miscible or immiscible with PLA, which resulted in the depression of the crystallization rate of PLA block. For the PBS block, its crystallization rate depended on the block length of PDLA, and the crystallization rate was the highest in the B-D 2-2 specimen, which differed from the cases of PEG[46] and PCL[36,47] blocks. The stronger nucleation ability could be due to the better lattice matching,[48] and the lattice matching between PLA and PBS was better[49,50] than that between PLA and PCL[51] or PEG.[52]

The Melting of PDLA Block

After crystallized at 90–140 °C and then at 70 °C, the second DSC

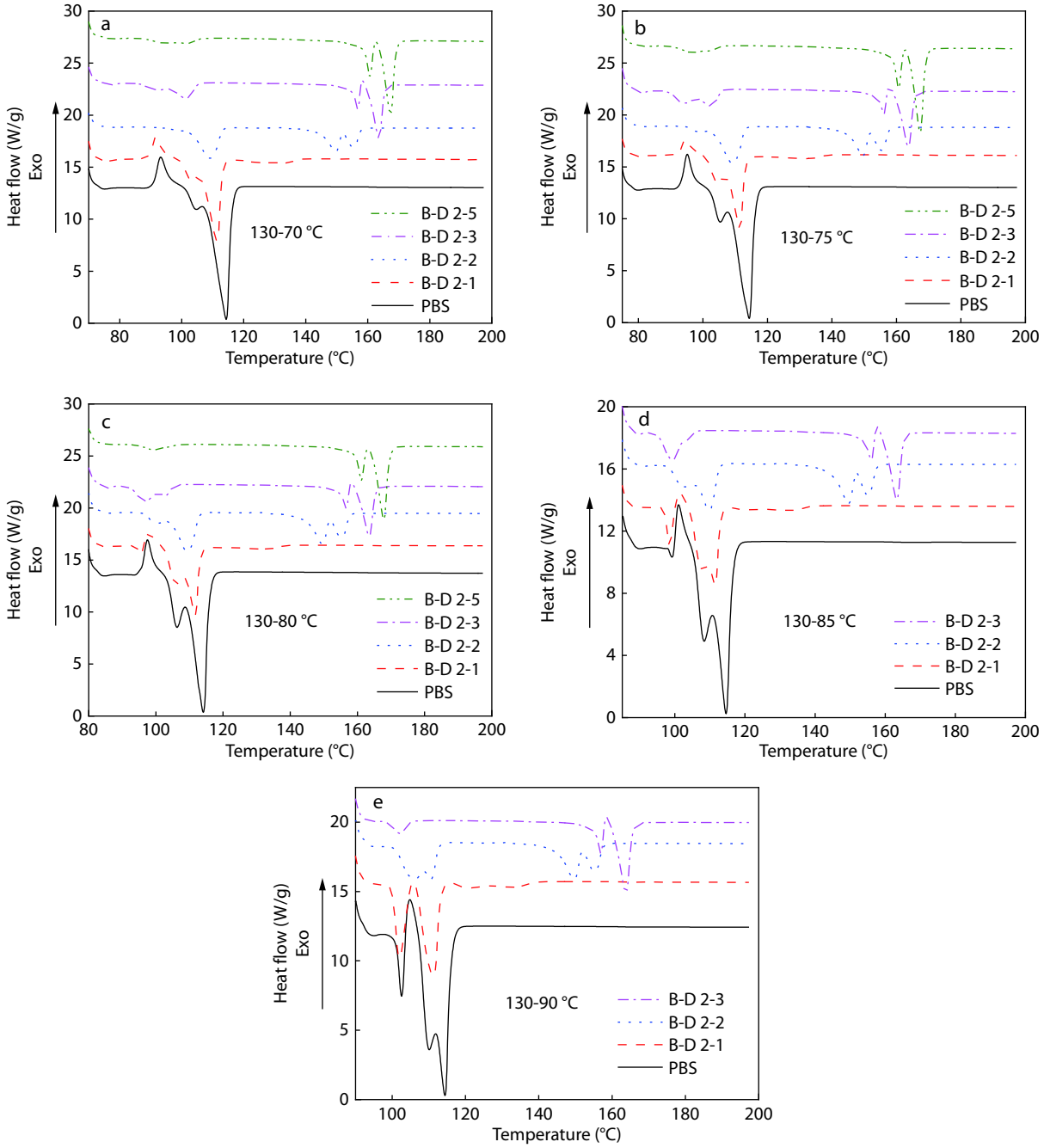

Fig. 8 The second DSC heating curves of block copolymers after crystallized first at 130 °C and then at 70 °C (a), 75 °C (b), 80 °C (c), 85 °C (d), and 90 °C (e).

https://doi.org/10.1007/s10118-020-2361-6

heating curves of all the specimens were recorded as shown in Fig. 7. For B-D 2-1 (Fig. S6 in ESI), a tiny board endothermic peak was detected at ~120 °C, which was assigned to the melting of PDLA block. After a higher content of PDLA was incorporated into the block copolymer, the melting signals belonging to PDLA block were enhanced and their melting temperature increased (Figs. 7a–7d). The PDLA block presented multiple melting behaviors, and an exothermic signal was found before the melting signals in the curves. For the original exothermic peak before the melting peak, it was assigned to the solid-solid transformation of PLA δ to α crystallites.[53] The multiple melting peaks of PDLA block were interpreted as that its crystallization was embarrassed by the PBS block; crystallites with different perfection degrees were produced during crystallization, and these imperfect crystallites were melted and recrystallized during heating.[54–56]

The Melting of PBS Block

After crystallized at 130 °C at the first stage and crystallized at 70–90 °C for 1 h subsequently, the second DSC heating curves were recorded as displayed in Fig. 8. In these DSC curves, the melting of PBS and PBS block exhibited multiple melting peaks. As the block length of PDLA increased, the melting signals assigned to PBS reduced. Increasing crystallization temperature, the melting temperature of PBS increased gradually.

CONCLUSIONS

In this study, a series of PDLA-*b*-PBS-*b*-PDLA triblock copolymers were synthesized, and the isothermal crystallization and subsequently melting behaviors of PDLA and PBS blocks were investigated.

In the case of PDLA block, crystallization signals were detected in the B-D 2-2 specimen, and the signals became stronger as a longer PDLA block was introduced into the copolymer. The crystallization rate was the highest in the B-D 2-2 specimen when crystallized at 90 and 100 °C. At higher crystallization temperature, the crystallization rate increased at first and then decreased as a longer PDLA block was incorporated. With the longer PDLA block covalently bonded to PBS, the crystallization enthalpy increased before leveling off, and the melting temperature increased gradually. The crystallization rate of PDLA in the tir-block copolymer was lower than that of PLA homopolymer.

For the PBS block, its crystallization behavior depended on nucleation and confinement. The crystallization and melting enthalpies of PBS block reduced gradually as a higher content of PDLA was incorporated. The crystallization rate decreased after a small amount of amorphous PDLA incorporated and reached the highest in the specimen of B-D 2-2. After a longer PDLA block was introduced, the PBS crystallites developed in a harsh environment. Elevating crystallization temperature, the crystallization rate was depressed, and more crystallites were developed with a low-dimensional structure.

Electronic Supplementary Information

Electronic supplementary information (ESI) is available free of charge in the online version of this article at http://dx.doi.org/10.1007/s10118-020-2361-6.

ACKNOWLEDGMENTS

This work was financially supported by the National Natural Science Foundation of China (Nos. 51403089, 51373169, 21574060, and 21374044), the Major Special Projects of Jiangxi Provincial Department of Science and Technology (No. 20114ABF05100), the Project of Jiangxi Provincial Department of Education (No. GJJ170229), the Technology Plan Landing Project of Jiangxi Provincial Department of Education (No. GCJ2011-243), the Outstanding Youth Foundation of Jiangxi Normal University, China Postdoctoral Science Foundation (No. 2019M652282), and Postdoctoral Science Foundation of Jiangxi Province (No. 2018KY37).

REFERENCES

1 Madhavan Nampoothiri, K.; Nair, N. R.; John, R. P. An overview of the recent developments in polylactide (PLA) research. *Bioresource Technol.* **2010**, *101*, 8493–8501.
2 Inkinen, S.; Hakkarainen, M.; Albertsson, A. C.; Södergård, A. From lactic acid to poly(lactic acid) (PLA): characterization and analysis of PLA and its precursors. *Biomacromolecules* **2011**, *12*, 523–532.
3 Jem, K. J.; van der Pol, J.; de Vos, S. Microbial lactic acid, its polymer poly(lactic acid), and their industrial applications. In *Plastics from Bacteria*, Ed. by Chen, G. G. Q. Springer Berlin Heidelberg, **2010**, Vol. 14, pp. 323–346.
4 Pang, X.; Zhuang, X.; Tang, Z.; Chen, X. Polylactic acid (PLA): research, development and industrialization. *Biotechnol. J.* **2010**, *5*, 1125–1136.
5 Saeidlou, S.; Huneault, M. A.; Li, H.; Park, C. B. Poly(lactic acid) crystallization. *Prog. Polym. Sci.* **2012**, *37*, 1657–1677.
6 Xu, J.; Guo, B. H. Poly(butylene succinate) and its copolymers: research, development and industrialization. *Biotechnol. J.* **2010**, *5*, 1149–1163.
7 Gigli, M.; Fabbri, M.; Lotti, N.; Gamberini, R.; Rimini, B.; Munari, A. Poly(butylene succinate)-based polyesters for biomedical applications: a review. *Eur. Polym. J.* **2016**, *75*, 431–460.
8 Deng, Y.; Thomas, N. L. Blending poly(butylene succinate) with poly(lactic acid): ductility and phase inversion effects. *Eur. Polym. J.* **2015**, *71*, 534–546.
9 Wuk, P. J.; Soon, I. S. Phase behavior and morphology in blends of poly(L-lactic acid) and poly(butylene succinate). *J. Appl. Polym. Sci.* **2002**, *86*, 647–655.
10 Wu, D.; Yuan, L.; Laredo, E.; Zhang, M.; Zhou, W. Interfacial properties, viscoelasticity, and thermal behaviors of poly(butylene succinate)/polylactide blend. *Ind. Eng. Chem. Res.* **2012**, *51*, 2290–2298.
11 Yokohara, T.; Yamaguchi, M. Structure and properties for biomass-based polyester blends of PLA and PBS. *Eur. Polym. J.* **2008**, *44*, 677–685.
12 Stoyanova, N.; Paneva, D.; Mincheva, R.; Toncheva, A.; Manolova, N.; Dubois, P.; Rashkov, I. Poly(L-lactide) and poly(butylene succinate) immiscible blends: from electrospinning to biologically active materials. *Mater. Sci. Eng. C* **2014**, *41*, 119–126.
13 Olivier, P.; Robert, Q.; Yahia, L.; John, S.; Stuart, M.; Leïla, B.; Philippe, D. Reactive compatibilization of poly(L-lactide)/poly(butylene succinate) blends through polyester maleation: From materials to properties. *Polym. Int.* **2014**, *63*, 1724–1731.

14 Chen, G. X.; Kim, H. S.; Kim, E. S.; Yoon, J. S. Compatibilization-like effect of reactive organoclay on the poly(L-lactide)/poly(butylene succinate) blends. *Polymer* **2005**, *46*, 11829–11836.
15 Tadashi, Y.; Kenzo, O.; Masayuki, Y. Effect of the shape of dispersed particles on the thermal and mechanical properties of biomass polymer blends composed of poly(L-lactide) and poly(butylene succinate). *J. Appl. Polym. Sci.* **2010**, *117*, 2226–2232.
16 Zhang, X.; Zhang, Y. Reinforcement effect of poly(butylene succinate) (PBS)-grafted cellulose nanocrystal on toughened PBS/polylactic acid blends. *Carbohyd. Polym.* **2016**, *140*, 374–382.
17 Masaki, H.; Tsubasa, O.; Kouji, I.; Hideki, H.; Koji, H.; Hiroyuki, F. Increased impact strength of biodegradable poly(lactic acid)/poly(butylene succinate) blend composites by using isocyanate as a reactive processing agent. *J. Appl. Polym. Sci.* **2007**, *106*, 1813–1820.
18 Zhang, B.; Bian, X.; Xiang, S.; Li, G.; Chen, X. Synthesis of PLLA-based block copolymers for improving melt strength and toughness of PLLA by *in situ* reactive blending. *Polym. Degrad. Stab.* **2017**, *136*, 58–70.
19 Valerio, O.; Misra, M.; Mohanty, A. K. Statistical design of sustainable thermoplastic blends of poly(glycerol succinate-*co*-maleate) (PGSMA), poly(lactic acid) (PLA) and poly(butylene succinate) (PBS). *Polym. Test.* **2018**, *65*, 420–428.
20 Supthanyakul, R.; Kaabbuathong, N.; Chirachanchai, S. Poly(L-lactide-*b*-butylene succinate-*b*-L-lactide) triblock copolymer: a multi-functional additive for PLA/PBS blend with a key performance on film clarity. *Polym. Degrad. Stab.* **2017**, *142*, 160–168.
21 Supthanyakul, R.; Kaabbuathong, N.; Chirachanchai, S. Random poly(butylene succinate-*co*-lactic acid) as a multi-functional additive for miscibility, toughness, and clarity of PLA/PBS blends. *Polymer* **2016**, *105*, 1–9.
22 Liu, Y.; Shao, J.; Sun, J.; Bian, X.; Chen, Z.; Li, G.; Chen, X. Toughening effect of poly(D-lactide)-*b*-poly(butylene succinate)-*b*-poly(D-lactide) copolymers on poly(L-lactic acid) by solution casting method. *Mater. Lett.* **2015**, *155*, 94–96.
23 Kawai, T.; Rahman, N.; Matsuba, G.; Nishida, K.; Kanaya, T.; Nakano, M.; Okamoto, H.; Kawada, J.; Usuki, A.; Honma, N. Crystallization and melting behavior of poly(L-lactic acid). *Macromolecules* **2007**, *40*, 9463–9469.
24 Li, S. Non-isothermal crystallization kinetics of poly(L-lactide). *Polym. Int.* **2010**, *59*, 1616.
25 Xiang, S.; Jun, S.; Li, G.; Bian, X. C.; Feng, L. D.; Chen, X. S.; Liu, F. Q.; Huang, S. Y. Effects of molecular weight on the crystallization and melting behaviors of poly(L-lactide). *Chinese J. Polym. Sci.* **2016**, *34*, 69–76.
26 Liu, X. Q.; Li, C. C.; Zhang, D.; Xiao, Y. N. Melting behaviors, crystallization kinetics, and spherulitic morphologies of poly(butylene succinate) and its copolyester modified with rosin maleopimaric acid anhydride. *J. Polym. Sci., Part B: Polym. Phys.* **2006**, *44*, 900–913.
27 Gan, Z.; Abe, H.; Kurokawa, H.; Doi, Y. Solid-state microstructures, thermal properties, and crystallization of biodegradable poly(butylene succinate) (PBS) and its copolyesters. *Biomacromolecules* **2001**, *2*, 605–613.
28 Park, J. W.; Kim, D. K.; Im, S. S. Crystallization behaviour of poly(butylene succinate) copolymers. *Polym. Int.* **2002**, *51*, 239–244.
29 Park, S. B.; Hwang, S. Y.; Moon, C. W.; Im, S. S.; Yoo, E. S. Plasticizer effect of novel PBS ionomer in PLA/PBS ionomer blends. *Macromol. Res.* **2010**, *18*, 463–471.
30 Pivsa-Art, W.; Fujii, K.; Nomura, K.; Aso, Y.; Ohara, H.; Yamane, H. Isothermal crystallization kinetics of talc-filled poly(lactic acid) and poly(butylene succinate) blends. *J. Polym. Res.* **2016**, *23*, 144.
31 Ba, C.; Yang, J.; Hao, Q.; Liu, X.; Cao, A. Syntheses and physical characterization of new aliphatic triblock poly(L-lactide-*b*-butylene succinate-*b*-L-lactide)s bearing soft and hard biodegradable building blocks. *Biomacromolecules* **2003**, *4*, 1827–1834.
32 Lan, X.; Li, X.; Liu, Z.; He, Z.; Yang, W.; Yang, M. Composition, morphology and properties of poly(lactic acid) and poly(butylene succinate) copolymer system *via* coupling reaction. *J. Macromol. Sci.* **2013**, *50*, 861–870.
33 Lin, J.; Yin, L. Z.; Li, Y.; Li, Q. B.; Yang, J.; Yu, J. Y.; Shi, Z.; Fang, Q.; Cao, A. New enantiomeric polylactide-block-poly(butylene succinate)-block-polylactides: syntheses, characterization and in situ self-assembly. *Macromol. Biosci.* **2005**, *5*, 526–538.
34 Zeng, J. B.; Li, Y. D.; Zhu, Q. Y.; Yang, K. K.; Wang, X. L.; Wang, Y. Z. A novel biodegradable multiblock poly(ester urethane) containing poly(L-lactic acid) and poly(butylene succinate) blocks. *Polymer* **2009**, *50*, 1178–1186.
35 Müller, A. J.; Balsamo, V.; Arnal, M. L. Nucleation and crystallization in diblock and triblock copolymers. In *Block copolymers II*, Abetz, V., 1st Ed. Springer Berlin Heidelberg, Berlin, Heidelberg, **2005**, pp. 1–63.
36 Castillo, R. V.; Müller, A. J.; Raquez, J. M.; Dubois, P. Crystallization kinetics and morphology of biodegradable double crystalline PLLA-*b*-PCL diblock copolymers. *Macromolecules* **2010**, *43*, 4149–4160.
37 Castillo, R. V.; Müller, A. J. Crystallization and morphology of biodegradable or biostable single and double crystalline block copolymers. *Prog. Polym. Sci.* **2009**, *34*, 516–560.
38 Zhou, D.; Shao, J.; Li, G.; Sun, J.; Bian, X.; Chen, X. Crystallization behavior of PEG/PLLA block copolymers: effect of the different architectures and molecular weights. *Polymer* **2015**, *62*, 70–76.
39 Chen, C. H.; Peng, J. S.; Chen, M.; Lu, H. Y.; Tsai, C. J.; Yang, C. S. Synthesis and characterization of poly(butylene succinate) and its copolyesters containing minor amounts of propylene succinate. *Colloid Polym. Sci.* **2010**, *288*, 731–738.
40 Shao, J.; Tang, Z. H.; Sun, J. R.; Li, G.; Chen, X. S. Linear and four-armed poly(L-lactide)-block-poly(D-lactide) copolymers and their stereocomplexation with poly(lactide)s. *J. Polym. Sci., Part B: Polym. Phys.* **2014**, *52*, 1560–1567.
41 Avrami, M. Kinetics of phase change. II. Transformation-time relations for random distribution of nuclei. *J. Chem. Phys.* **1940**, *8*, 212–224.
42 Avrami, M. Kinetics of phase change. I. General theory. *J. Chem. Phys.* **1939**, *7*, 1103–1112.
43 Yin, H. Y.; Wei, X. F.; Bao, R. Y.; Dong, Q. X.; Liu, Z. Y.; Yang, W.; Xie, B. H.; Yang, M. B. High-melting-point crystals of poly(L-lactic acid) (PLLA): the most efficient nucleating agent to enhance the crystallization of PLLA. *CrystEngComm* **2015**, *17*, 2310–2320.
44 Huang, C. I.; Tsai, S. H.; Chen, C. M. Isothermal crystallization behavior of poly(L-lactide) in poly(L-lactide)-block-poly(ethylene glycol) diblock copolymers. *J. Polym. Sci., Part B: Polym. Phys.* **2006**, *44*, 2438–2448.
45 Yang, J.; Zhao, T.; Liu, L.; Zhou, Y.; Li, G.; Zhou, E.; Chen, X. Isothermal crystallization behavior of the poly(L-lactide) block in poly(L-lactide)-poly(ethylene glycol) diblock copolymers: influence of the PEG block as a diluted solvent. *Polym. J.* **2006**, *38*, 1251–1257.
46 Yang, J.; Zhao, T.; Cui, J.; Liu, L.; Zhou, Y.; Li, G.; Zhou, E.; Chen, X. Nonisothermal crystallization behavior of the poly(ethylene

https://doi.org/10.1007/s10118-020-2361-6

glycol) block in poly(L-lactide)-poly(ethylene glycol) diblock copolymers: Effect of the poly(L-lactide) block length. *J. Polym. Sci., Part B: Polym. Phys.* **2006**, *44*, 3215–3226.
47 Hamley, I. W.; Castelletto, V.; Castillo, R. V.; Müller, A. J.; Martin, C. M.; Pollet, E.; Dubois, P. Crystallization in poly(L-lactide)-*b*-poly(ε-caprolactone) double crystalline diblock copolymers: a study using X-ray scattering, differential scanning calorimetry, and polarized optical microscopy. *Macromolecules* **2005**, *38*, 463–472.
48 Hu, J.; Xin, R.; Hou, C. Y.; Yan, S. K.; Liu, J. C. Direct comparison of crystal nucleation activity of PCL on patterned substrates. *Chinese J. Polym. Sci.* **2019**, *37*, 693–699.
49 Okihara, T.; Tsuji, M.; Kawaguchi, A.; Katayama, K. I.; Tsuji, H.; Hyon, S. H.; Ikada, Y. Crystal structure of stereocomplex of poly(L-lactide) and poly(D-lactide). *J. Macromol. Sci. Part B* **1991**, *30*, 119–140.
50 Ihn, K. J.; Yoo, E. S.; Im, S. S. Structure and morphology of poly(tetramethylene succinate) crystals. *Macromolecules* **1995**, *28*, 2460–2464.
51 Bittiger, H.; Marchessault, R. H.; Niegisch, W. D. Crystal structure of poly-ε-caprolactone. *Acta Cryst. B* **1970**, *26*, 1923–1927.
52 Takahashi, Y.; Tadokoro, H. Structural studies of polyethers, $(-(CH_2)_m-O-)_n$. X. Crystal structure of poly(ethylene oxide). *Macromolecules* **1973**, *6*, 672–675.
53 Zhang, J. M.; Duan, Y. X.; Sato, H.; Tsuji, H.; Noda, I.; Yan, S.; Ozaki, Y. Crystal modifications and thermal behavior of poly(L-lactic acid) revealed by infrared spectroscopy. *Macromolecules* **2005**, *38*, 8012–8021.
54 Michell, R. M.; Müller, A. J.; Spasova, M.; Dubois, P.; Burattini, S.; Greenland, B. W.; Hamley, I. W.; Hermida-Merino, D.; Cheval, N.; Fahmi, A. Crystallization and stereocomplexation behavior of poly(D- and L-lactide)-*b*-poly(*N*,*N*-dimethylamino-2-ethyl methacrylate) block copolymers. *J. Polym. Sci., Part B: Polym. Phys.* **2011**, *49*, 1397–1409.
55 Sarasua, J. R.; Prud'homme, R. E.; Wisniewski, M.; Le Borgne, A.; Spassky, N. Crystallization and melting behavior of polylactides. *Macromolecules* **1998**, *31*, 3895–3905.
56 Di Lorenzo, M. L. Calorimetric analysis of the multiple melting behavior of poly(L-lactic acid). *J. Appl. Polym. Sci.* **2006**, *100*, 3145–3151.

https://doi.org/10.1007/s10118-020-2361-6